ISSN 0031-918X, Physics of Metals and Metallography, 2019, Vol. 120, No. 13, pp. 1266–1269. © Pleiades Publishing, Ltd., 2019.

Magneto-Optical Effects in Au/Ni Based Composite Hyperbolic Metamaterials

I. A. Kolmychek[a], *, A. R. Pomozov[a], A. P. Leontiev[a], K. S. Napolskii[a], and T. V. Murzina[a]

[a] *Moscow State University, Moscow, 119991 Russia*

**e-mail: irisha@shg.ru*

Received June 28, 2019

Abstract—The results of synthesis and experimental study of two types of nanocomposites based on Au/Ni nanorods in porous anodic alumina matrix are presented. The existence of two features in the optical spectra of such structures corresponding epsilon-near-zero and epsilon-near-pole points is shown. A significant modulation and enhancement of the alternating magneto-optical effects are observed in the spectral vicinity of these points.

Keywords: hyperbolic metamaterials, magneto-optical effects, epsilon-near-zero

DOI: 10.1134/S0031918X19130131

INTRODUCTION

Hyperbolic metamaterials (HMMs) are artificial media possessing strong uniaxial optical anisotropy characterized by effective permittivity tensor with principal components of the opposite signs for the directions corresponding parallel and perpendicular to the optical axis [1, 2]. The most popular configurations of HMMs are a metal-dielectric multilayer stack or an ordered array of metal nanowires in a dielectric host material. In both types of structures, the hyperbolic dispersion law is achievable in the optical range (instead of elliptical dispersion in traditional dielectrics) leading to a number of unusual optical properties that can find a plenty of applications, from high-resolution imaging and lithography [3, 4] to biosensing [5] and waveguiding [6]. Dispersion properties of the constituting materials along with the design of the HMMs provide two distinct pecularities of the spectra of their epsilon tensor components. The first one is a change in the sign of the real part of one of the components of the effective permittivity tensor and thus the appearance of Epsilon Near Zero (ENZ) point [7]. The second one is the pole of effective epsilon component (Epsilon Near Pole, ENP).

One of the efficient and convenient techniques for the HMMs fabrication is templated electrodeposition of a metal inside the cylindrical pores of anodic aluminum oxide (AAO) matrix. In such structures, two plasmon resonances (along and perpendicular to the nanorods axes) can be excited [8] providing resonant effects due to the amplification of the electric filed of the pump radiation.

A novel trend in the field of hyperbolic media studies is a combination of HMMs with gyrotropic materials [9]. Such composite structures are interesting from the fundamental point of view as novel effects can be revealed in the magneto-optical response in the spectral vicinity of the ENZ or ENP points. They also provide possibilities of the magnetic-field-assisted light manipulation perspective for the modern nanophotonics. It is worth noting that the plasmon-assisted enhancement of magneto-optical effects was already observed in a number of papers [10–12], whereas these experiments were performed far from the ENZ and hyperbolic dispersion spectral regions.

Here, we present the experimental studies of optical and magneto-optical effects in two types of composite HMMs: (i) arrays of gold nanorods in AAO template supplemented by a continuous nickel film and (ii) composite gold/nickel nanorods in AAO.

SAMPLES AND EXPERIMENTAL SETUP

Arrays of gold nanorods in AAO matrices were prepared by templated electrodeposition. Detailed procedure was described in [13]. According to the SEM studies, the diameter of Au nanorods is about 40–50 nm and their length is about 500 nm, the volume fraction of gold in the nanocomposite being 8–10%. The volume fraction of the metal f_m strongly determines the functional properties of the nanocomposite. To fabricate HMMs of type (i) with f_m smaller than the template porosity, the controlled blocking of the portion of pores during anodization in 0.3 M $H_2C_2O_4$ was performed [14]. In the case of HMMs of type (ii), AAO matrices were prepared in 0.3 M H_2SeO_4 at 48 V and 0°C [15, 16]. This kind of AAO templates possess low porosity of ca. 8–10%.

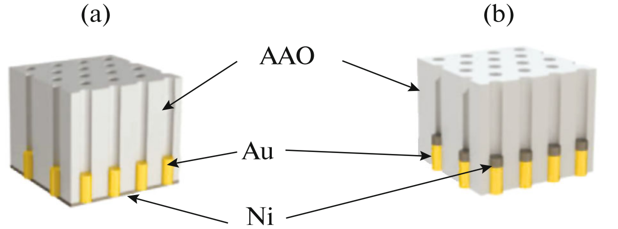

Fig. 1. Schemes of the samples under study.

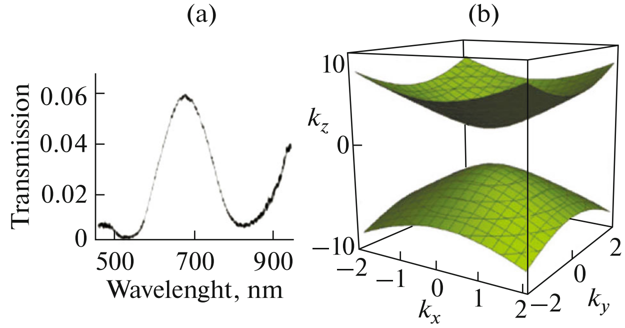

Fig. 2. (a) Transmission spectrum of the first-type sample measured for the angle of incidence 45°; (b) isofrequency surface for the sample at the wavelength $\lambda = 900$ nm. The components of the wave vector are indicated in the units of $2\pi/\lambda$.

In the first type of samples, a continuous nickel film of the thickness of about 15 nm was deposited onto one side of the template by DC magnetron sputtering, providing a contact with the vertically aligned Au nanorods (see Fig. 1a). In the second type of structures, nickel nanorods of 50 nm in length were formed above the gold ones (see Fig. 1b) by Ni electrodeposition at constant potential of −0.9 V versus Ag/AgCl reference electrode at room temperature from the electrolyte containing 0.7 M $NiSO_4$ and 0.3 M H_3BO_3.

For the optical spectroscopic studies, a halogen lamp was used as the source of a broadband light, the polarizer was installed to control the *p*-polarization of the incident light. Transmitted light was detected by a spectrometer. In the magneto-optical experiments, a DC magnetic field of 1 kOe formed by two permanent ring magnets was applied in the Faraday, Voight or Kerr geometries. The magneto-optical effect was measured through the magnetic contrast of the transmission as:

$$\rho = \frac{T(H) - T(-H)}{T(H) + T(-H)}, \quad (1)$$

where $T(\pm H)$ is transmittance of the structure for the opposite directions of the applied magnetic field, H. In the experiments in the Faraday geometry, an analyzer was set at 45° with respect to *p*-polarization, which allowed to reveal the polarization plane rotation. In the Voight geometry the total transmittance was detected. For the transversal Kerr geometry the magnetic contrast was calculated analogously to (1) when using the reflection data instead of the transmission ones. It should be noted that ellipticity of the transmitted light cannot be neglected as the birefringence is very strong [17] and the Faraday polarization plane rotation cannot be directly estimated from the value of magnetic contrast, as frequently can be performed for ferromagnetic films. As a reference structure without hyperbolic dispersion we used an AAO template without gold nanorods with a 15 nm-thick Ni continuous film deposited above.

EXPERIMENTAL RESULTS

The transmission spectrum of the sample of the first type HMM is shown in Fig. 2a. Two minima centered at the wavelengths of 540 and 820 nm are observed, which correspond to transversal and longitudinal plasmon resonances, respectively. The calculations of the effective permittivity components showed that these two resonances correspond to the pole of the component perpendicular to the nanorods $\varepsilon_\perp$ (ENP) and the sign reversal of the permittivity component along the nanorods $\varepsilon_\parallel$ [13]. Hyperbolic dispersion regime can be achieved at the wavelengths $\lambda > 820$ nm. For example, Fig. 2b demonstrates an isofrequency surface for $\lambda = 900$ nm. Previous studies showed that at this wavelength $\varepsilon_{xx} = \varepsilon_{yy} = \varepsilon_\perp = 4.2$, $\varepsilon_{zz} = \varepsilon_\parallel = -0.5$ [13], so that the isofrequency surface for the *k*-vector components in the units of $2\pi/\lambda$ has the form of hyperboloid.

It should be noted here that the presence of magnetic materials does not change significantly the nonmagnetic optical properties of the samples, while it decreases the overall transmission. Transmission spectrum of the second-type sample is qualitatively similar to that shown in Fig. 2a.

Figure 3a represents the spectra of ρ measured in the Faraday geometry for different angles of incidence. Two features should be pointed out here. The first one is a peak centered at approximately 540 nm with the quality factor decreasing with increasing the angle of incidence θ. The maximal value of the magnetic contrast is about 1.5×10^{-2} that exceeds by an order of magnitude the corresponding value for the reference nickel film. The second spectral feature is observed in the spectral region 770–970 nm and has a complicated oscillating behavior. Importantly that the magnetic contrast increases in this spectral region with the angle of incidence.

The spectrum of the magnetic contrast in the Voight geometry of Au nanorods array with Ni film is shown in Fig. 3b. It reveals an amplification along with the sign reversal of ρ in the spectral vicinity of the

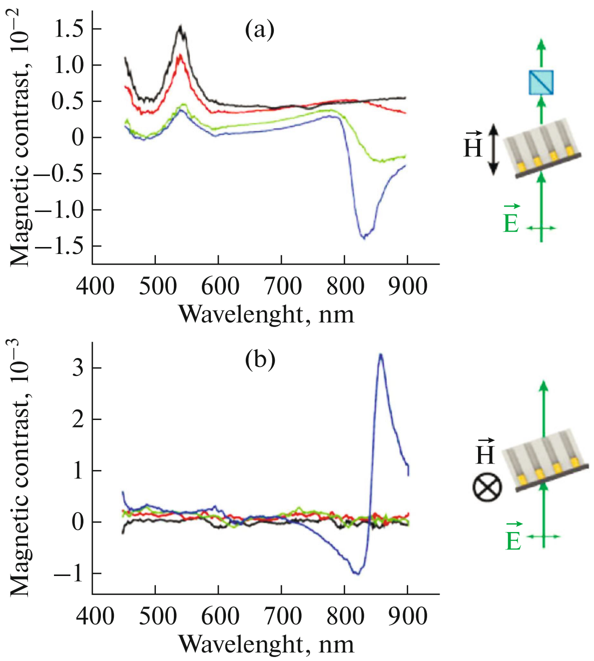

Fig. 3. Spectra of the magnetic contrast measured for the sample of the first type in the Faraday (a) and the Voight (b) geometry for different angles of incidence: 0° (black lines), 20° (red lines), 30° (green lines), and 35° (blue lines). Schemes of the experiments are shown in the right panels.

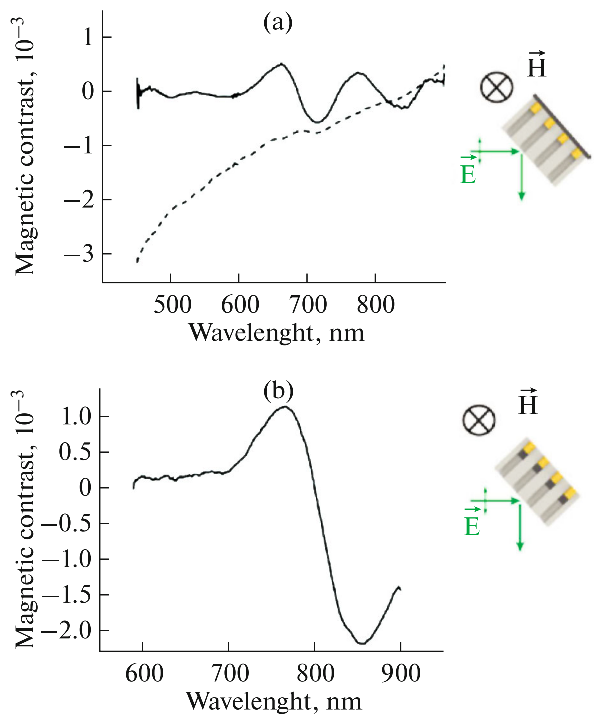

Fig. 4. Spectra of the magnetic contrast measured in transversal Kerr geometry for the sample of the first type (a) and second type (b) for the angle of incidence of 45° (solid lines). Analogous spectrum for the reference nickel film is shown in the panel (a) by dashed line. Schemes of the experiments are shown in the right panels.

ENZ point $\lambda = 820$ nm for the angle of incidence $\theta = 35°$. For smaller angles of incidence, ρ is close to zero.

Figure 4 shows the spectra of the magnetic contrast in the Kerr geometry for $\theta = 45°$. For both samples (solid lines) we observe alternating in the sign of magnetic contrast near the ENZ point. For the reference in Ni film (Fig. 4a, dashed line) the spectrum of ρ is monotonous. This confirms the principle role played by the HMM structure in the observed enhancement of the magneto-optical effects.

DISCUSSION

Optical properties of the composite HMM are defined by the components of effective permittivity tensor, corresponding to the directions perpendicular ($\varepsilon_{\perp}$) and parallel ($\varepsilon_{\parallel}$) to nanorods, which depend on the volume fraction of gold and the nanorods' length, whereas are slightly sensitive to the presence of small amount of additional magnetic materials. The amplification of ρ in the spectral vicinity of the ENP point occurs due to a strong electric field localization and enhancement of the light-matter interaction under the transversal plasmon resonance excitation (Fig. 3a). Similar effects were observed in non-hyperbolic magneto-plasmonic structures of various design [10, 11].

The spectra of the magneto-optical effects in the vicinity of the ENZ point in the nanocomposite consisting of Ni thin film and HMM are associated with the strong optical anisotropy of nanorods' array in this spectral region. In the Faraday geometry, *p*-polarized pump light falls onto the gyrotropic film that rotates the polarization plane [18]. So, after the Ni film, the polarization plane is slightly inclined with respect to the plane of incidence. The nanorods array screws it up due to the giant absorption anisotropy of the sample as well as due to the stong difference between phase velocities of the ordinary and extraordinary beams in the spectral vicinity of the ENZ point. This mechanism explains the enhancement, oscillating behaviour and the strong dependence of ρ on the angle of incidence near $\lambda = 820$ nm (Fig. 3a).

CONCLUSIONS

Optical properties of artificial composite structures that combine hyperbolic and magnetic materials of two designs were investigated. Spectra of the magneto-optical effects of the samples were studied for different angles of incidence of the probing radiation in a wide spectral region, which includes the specific epsilon-near-zero spectral points. It was found that the magneto-optical response of the HMM with ferromagnetic compounds is strongly enhanced and modulated close to these spectral regions, which is attributed to the light localization effects in the birefringent HMM. These results provide wide perspectives for the selective enhancement of the magneto-optical response.

FUNDING

The financial support of the President's grant MK-5704.2018.2 is greatly acknowledged. A.R.P. also acknowledges the financial support of the Foundation for the advancement of theoretical physics and mathematics "BASIS".

REFERENCES

1. M. G. Silveirinha, "Nonlocal homogenization model for a periodic array of ε-negative rods," Phys. Rev. E **73**, 046612 (2006).
2. A. Poddubny, I. Iorsh, P. Belov, and Y. Kivshar, "Hyperbolic metamaterials," Nature Photonics **7**, 948–957 (2013).
3. J. Sun M. I. Shalaev, and N. M. Litchinitser, "Experimental demonstration of a non-resonant hyperlens in the visible spectral range," Nature Commun. **6**, 7201 (2015).
4. T. Li, V. Nagal, D. H. Gracias, and J. B. Khurgin, "Limits of imaging with multilayer hyperbolic metamaterials," Optics Express **25**, 13588–13601 (2017).
5. K. V. Sreekanth, M. ElKabbash, Y. Alapan, E. I. Ilker, M. Hinczewski, U. A. Gurkan, and G. Strangi, "Hyperbolic metamaterials-based plasmonic biosensor for fluid biopsy with single molecule sensitivity," EPJ Appl. Metamat. **4**, 1–8 (2017).
6. N. Vasilantonakis, M. E. Nasir, W. Dickson, G. A. Wurtz, and A. V. Zayats, "Bulk plasmon-polaritons in hyperbolic nanorod metamaterial waveguides," Laser Phot. Rev. **9**, 345–353 (2015).
7. L. Ferrari, Ch. Wu, D. Lepage, X. Zhang, and Z. Liu, "Hyperbolical metamaterials and their applications," Prog. Quant. Electronics **40**, 1–40 (2015).
8. R. Atkinson, W. R. Hendren, G. A. Wurtz, W. Dickson, A. V. Zayats, P. Evans, and R. J. Pollard, "Anisotropic optical properties of arrays of gold nanorods embedded in alumina," Phys. Rev B **73**, 235402 (2006).
9. B. Fan, M. E. Nasir, L. H. Nicholls, A. V. Zayats, and V. A. Podolskiy, "Magneto-optical metamaterials: Nonreciprocal transmission and Faraday effect enhancement," Adv. Opt. Mater. **7**, 1801420 (2019).
10. J. B. Gonzalez-Diaz, A. Garcia-Martin, J. M. Garcia-Martin, A. Cebollada, G. Armelles, B. Sepúlveda, Y. Alaverdyan, M. Käll, "Plasmonic Au/Co/Au nanosandwiches with enhanced magneto-optical activity," Small **4** (2), 202–205 (2008).
11. M.Abe and T. Suwa, "Surface plasma resonance and magneto-optical enhancement in composites containing multicore-shell structured nanoparticles," Phys. Rev. B **70**, 235103 (2004).
12. I. A. Kolmychek, A. N. Shaimanov, A. V. Baryshev, and T. V. Murzina, "Magneto-optical response of two-dimensional magnetic plasmon structures based on gold nanodisks embedded in a ferrite garnet layer," JETP Lett. **102**, 46–50 (2015).
13. I. A. Kolmychek, A. R. Pomozov, A. P. Leontiev, K. S. Napolskii, and T. V. Murzina, "Magneto-optical effects in hyperbolic metamaterials," Opt. Lett. **43**, 3917–3920 (2018).
14. A. P. Leontiev, O. Yu. Volkova, I. A. Kolmychek, A. V. Venets, A. R. Pomozov, V. S. Stolyarov, T. V. Murzina, and K. S. Napolskii, "Tuning the optical properties of hyperbolic metamaterials via volume fraction of metallic nanorods," Nanomaterials **9**, 739–749 (2019).
15. F. O. Gordeeva, I. V. Roslyakov, and K. S. Napolskii, "Aluminium anodizing in selenic acid: electrochemical behaviour, porous structure, and ordering regimes," Electrochem. Acta **307**, 13–19 (2019).
16. O. Nishinaga, T. Kikuchi, S. Natsui, and R. O. Suzuki, "Rapid fabrication of self-ordered porous alumina with 10-/sub-10-nm-scale nanostructures by selenic acid anodizing," Sci. Rep. **3**, 2748 (2013).
17. P. Ginzburg, F. J. R. Fortuno, G. A. Wurtz, W. Dickson, A. Murphy, F. Morgan, R. J. Pollard, I. Iorsh, A. Atrashchenko, P. A. Belov, Y. S. Kivshar, A. Nevet, G. Ankonina, M. Orenstein, and A. V. Zayats, "Manipulating polarization of light with ultrathin epsilon-near-zero metamaterials," Optics Express **21**, 14907–14917 (2013).
18. K. Zvezdin and V. A. Kotov, *Modern Magnetooptics and Magnetooptical Materials* (Institute of Physics, Bristol and Philadelphia, 1997.